Bitlis Eren Üniversitesi Fen Bilimleri Dergisi
BİTLİS EREN UNIVERSITY JOURNAL OF SCIENCE
ISSN: 2147-3129/e-ISSN: 2147-3188
VOLUME: 12 NO: 3 PAGE: 887-893 YEAR: 2023
DOI:10.17798/bitlisfen.1333113

Determination of Energy Absorption Capabilities of Shear Thickening Fluid Impregnated Aramid Fiber Fabrics for Ballistic Applications

Ali İmran AYTEN[1*]

[1]*Yalova University, Faculty of Engineering, Department of Polymer Materials Engineering, Yalova, 77200, TURKEY*
(ORCID: 0000-0002-3948-3690)

Keywords: Drop weight impact test, Energy absorption capability, Shear thickening fluid, Para-aramid fabric.

Abstract

The low-velocity impact behavior of shear thickening fluid (STF) impregnated aramid fabric having different numbers of layers was investigated throughout this study to determine a relationship between the number of layers and perforation energy. Firstly, STF solutions, including polyethylene glycol, silica nanoparticles, and ethanol, were prepared by mixing with a homogenizer. Solutions containing 5%, 10%, and 20% silica nanoparticles by weight were prepared, and rheological analysis was performed. 20% weight fraction solution showed the optimum thickening behavior among the three solutions. After thickening behavior and the critical shear rate were determined from rheological analysis, the solution was impregnated into the aramid fabric. Then, specimens with different numbers of layers, from 1 to 8, were prepared for low-velocity impact experiments. A drop-weight impact test was applied at different energy levels from 20 J to 240 J, and perforation energy was determined. Finally, an equation that has a form of power function was fitted to use it for potential energy absorption applications such as ballistic impact.

1. Introduction

Shear thickening fluids (STF) are the solutions in which nanoparticles are dispersed in a polymer phase. They can be defined as non-Newtonian fluids that do not follow Newton's viscosity law. In Newtonian fluids, viscosity remains constant as the shear rate increases, whereas in shear thickening fluids, viscosity increases with an increasing shear rate, and the fluid behaves like a solid for an instant. The fundamental reason for this behaviour is that the silica nanoparticles in STF are dispersed and homogeneous when no stress is applied. When the shear stress is applied, silica nanoparticles come together and show agglomeration behaviour, due to the polymer phase in the solution. There are various applications of shear thickening fluids in the literature [1]-[21]. One of the most common applications of STF is the impregnation of the aramid fabric to increase its energy absorption capability.

The first study on the impregnation of aramid fabric was conducted by Lee et al.[22]. STF, including silica nanoparticles with a diameter of 450 nm particles impregnated with woven Kevlar fabric, was tested by shooting with a bullet having a speed of 244 m/s. They found that the 2 ml STF-impregnated Kevlar fabric, consisting of 4 layers, showed 42% less deformation compared to the bare 4-layer Kevlar fabric.

Avila et al. [23] achieved a dual-phase formation by dispersing calcium carbonate and nanosilica fillers in polyethylene glycol (PEG) and ethanol, and they enabled the spread of these fillers into aramid fiber fabric. This method increased the inter-yarn friction and bullet deformation. They found that a composition of 25% nanosilica and 75% calcium carbonate by weight yielded the best results. They observed that the ballistic performance of a 32-layer aramid fabric was equivalent to that of a 19-

*Corresponding author: aiayten@yalova.edu.tr
Received: 26.07.2023, Accepted: 18.09.2023

layer aramid fabric impregnated with a nanosilica/calcium carbonate solution.

Gürgen and Kuşhan [24] synthesized multi-phase STFs by adding varying amounts of silicon carbide (SiC) to a silica- and PEG-based solution. They conducted ballistic tests on aramid fabrics impregnated with multi-phase STFs using lead-core bullets at a speed of 330 m/s. Rheology tests revealed that single-phase STF samples exhibited more thickening behavior compared to multi-phase STF samples. However, aramid fabrics impregnated with multi-phase STFs provided significant benefits, especially in reducing trauma depth. They mentioned that the potential drawback of multi-phase STF samples was their increased areal density.

In another study by Gürgen and Kuşhan [25], three different ceramic fillers, namely silicon carbide, aluminum oxide, and boron carbide, were added to STFs in various weight percentages within the composite. The researchers investigated the rheological effects of these added fillers on the STFs. They found that these additions significantly influenced the thickening behavior of the STFs. For instance, at 60°C and with a 5% weight of filler, the composite containing aluminum oxide exhibited the highest thickening behavior.

Khodadadi et al. [26] prepared STFs containing silica nanoparticles at weight percentages of 15%, 25%, 35%, and 45%. They examined the energy dissipation performance of solutions. In ballistic tests, they observed that fabric impregnated with STFs showed increased energy dissipation values, but STFs with a high percentage of nanosilica filler started to have negative effects. They determined that the specific energy dissipation value of the Kevlar fabric impregnated with 15% filler STFs was lower than that of the bare Kevlar fabric. On the other hand, the Kevlar fabric impregnated with 35% filler STFs exhibited a 2.3 times higher specific energy dissipation value compared to the neat Kevlar fabric.

Qin et al. [27] synthesized a new type of STF and impregnated it into Kevlar fabric, then subjected it to a dynamic penetration resistance test. They found that the new type of STF, containing silica microspheres and ionic liquid, exhibited a unique double-continuous shear thickening behavior. They achieved the optimum dynamic penetration resistance with 34.89% by weight of STF-impregnated fabric. They observed that the newly synthesized STF significantly increased inter-yarn friction.

In this study, three different solutions with different silica nanoparticle weight ratios (5%, 10%, and 20%) were prepared and their rheological behaviors were examined. According to the results, in the final step of the rheological analysis, STF with 20% silica concentration was prepared and soaked into aramid fabric. Additionally, 20% silica concentration is the optimum rate in most published studies because the high amount of silica in STF may create an agglomeration problem at the preparation stage of the fluid. After the impregnation process is completed, different numbers of layers of aramid fabric are subjected to a drop-weight impact test to determine their energy absorption capabilities. After determining the "number of layers-perforation energy" relationship, the equation was obtained by the curve fitting method. This equation may be used to determine how many layers of fabric are needed for ballistic protection at different ballistic protection levels.

2. Material and Method

Shear thickening fluid solution was prepared by using polyethylene glycol (PEG) 200 (Merck), ethanol, and hydrophilic fumed silica nanoparticles, which have a 12 nm diameter particle size (Aerosil 200, Evonik). First, PEG and ethanol were mixed by homogenizer (IKA T18 Basic Ultra Turrax) for 15 min at 3000-3500 rpm (Figure 1a). After they were completely mixed, Aerosil 200 silica nanoparticles were manually added to prevent agglomeration as the mixing continued. When the addition of silica nanoparticles was ended, mixing of all components continued for 1 h.

Three mixtures were prepared with three different Aerosil 200/PEG200 weight ratios, namely 5%, 10%, and 20%. STF solution was poured into a container, and aramid fabric was soaked into the solution (Figure 1b). Twaron CT709 plain weave aramid fabric (Teijin Ltd.), having a 200 g/m2 real weight, was used throughout this study. Both sides of the fabric were left in solution to provide impregnation for 2 min. The fabric was hung on the rope and left for 1 day to evaporate the ethanol (Figure 1c). Finally, specimens with two or more layers were stitched to prevent slipping throughout low-velocity impact experiments.

Rheology analysis was carried out by a rotational dynamic oscillatory hybrid rheometer (TA Instruments, Discovery HR-1) with 25 mm diameter parallel plates within a shear strain rate of 1 to 2250 s^{-1} at room temperature.

The Instron Ceast 9350 drop tower impact system was used to perform low-velocity impact (LVI) tests at different energy levels depending on the number of fabric layers. A series of LVI experiments

were performed from 1 layer to 8 layers of STF-impregnated aramid fabrics. A hemispherical impactor tip with 10 mm diameter was used as an impactor (Figure 2). Extra mass was added to adjust the impact energy. Different initial energies, from 20 J to 240 J, were set for different numbers of fabric layers.

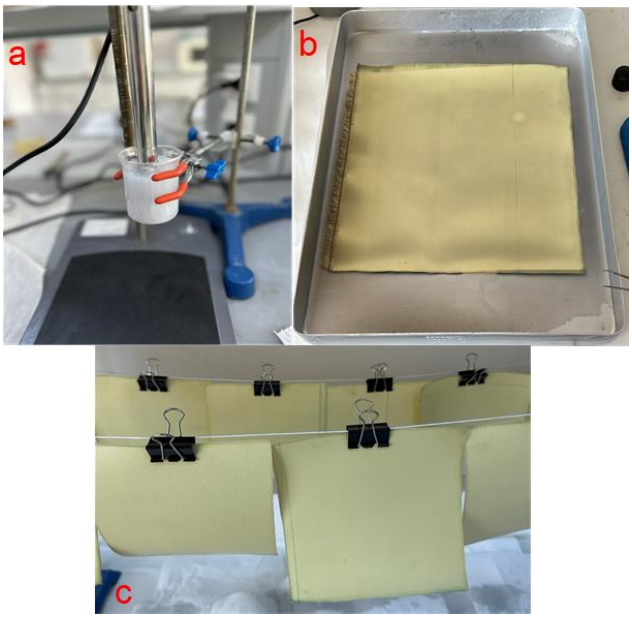

Figure 1. Preparation of STF and impregnate it to the aramid fabric. a) Mixing the solution components by homogenizer, b) Impregnation of the STF into the aramid fabric, c) Drying fabric for evaporating ethanol.

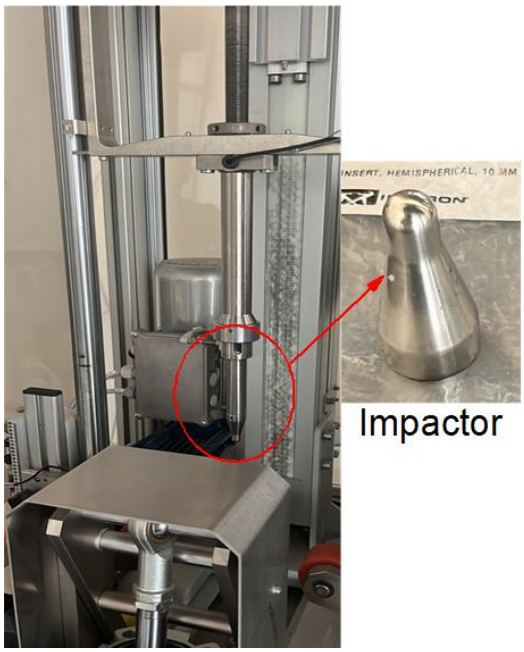

Figure 2. Drop tower impact system and impactor.

3. Results and Discussion

3.1. SEM Results

SEM images were captured to understand the impregnation of STF on the surface of aramid fiber. Figure 3 shows the images of neat and STF-impregnated fabric at different magnifications. When Figures 3a and 3b were compared, the difference between two of them could be clearly observed. The surface of the aramid fibers was covered by the STF solution. Herein, PEG plays a crucial role in sticking to the surface. Figures 3c and 3d have a difference in terms of the fabric being covered by STF homogeneously.

3.2. Rheological Analysis Result

Rheological analysis was carried out with an increasing shear rate between 1 and 2250 s^{-1}. PEG has a Newtonian characteristic, but its behavior has been changing by adding silica nanoparticles [24]. In Figure 4, the viscosity curve includes three zones according to the viscosity change. Firstly, the solution showed a thinning behavior until the 250 s^{-1} shear rate value, and then shear thickening behavior was observed because silica nanoparticles aggregated in the polymer phase. At the final step, agglomerated parts of nanoparticles suddenly crashed at the high shear rate, and shear thinning behavior was observed again.

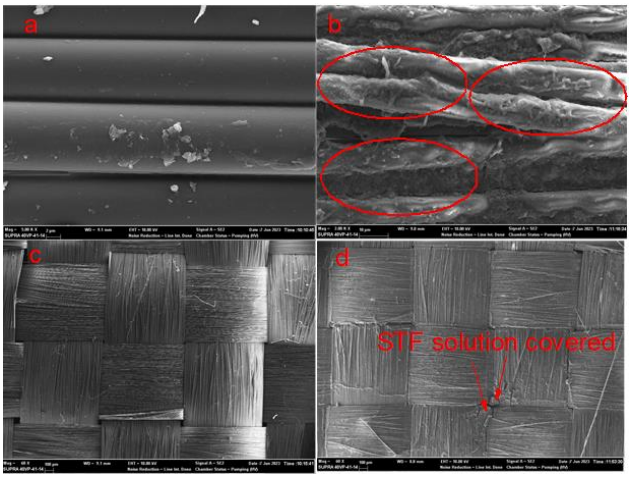

Figure 3. SEM images of a) neat fabric at 2 µm scale, b) STF impregnated fabric at 10 µm scale, c) neat fabric at 100 µm scale, d) STF impregnated fabric at 100 µm scale.

Figure 5 presents a comparison of different solutions, including different amounts of silica nanoparticles. The 5% silica concentration solution did not show any thickening behaviour. Its viscosity

increased 0.74 times between 6.42 and 1534.78 s^{-1} shear rates. The viscosity value of a 10% silica concentration solution increased 9.575 times (957.5%) between 100 and 250 s^{-1} shear rate values. The greatest viscosity increase was observed in the 20% solution. It showed viscosity increasing 11.02 times (1102%) between 100 and 640.37 s^{-1} shear rate.

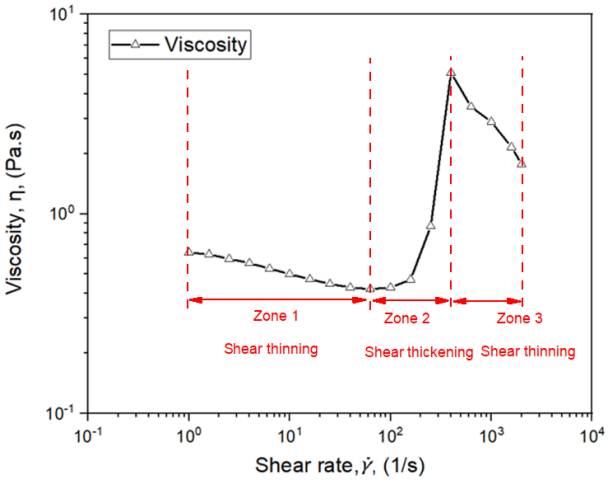

Figure 4. Viscosity-shear rate relationship for Aerosil 200/PEG 200 STF solution.

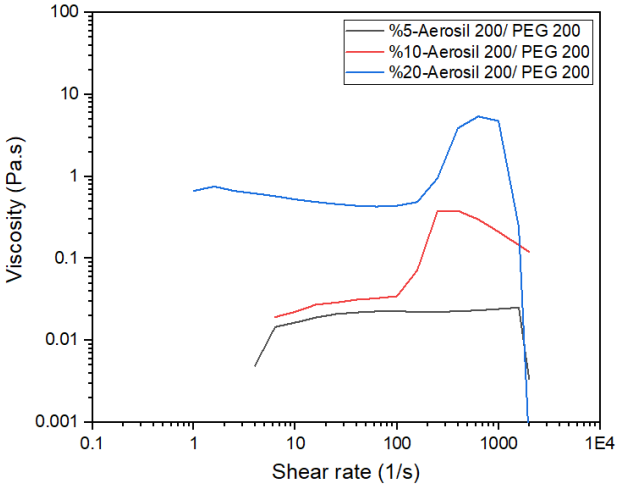

Figure 5. Comparison of Aerosil 200/PEG200 solution at different silica nanoparticle concentrations.

3.3. Low Velocity Impact Test Results

Figure 6 compares the low-velocity impact response of 3 layers of neat and STF-impregnated aramid fabric. There is an 18.5% difference in terms of maximum loading. Figure 7 presents force-displacement curves for 1 layer to 8 layers of aramid fabric. The curves include noise because the soft structure of the fabric causes contact problems between the impactor and the specimen. When the first 10 mm displacement value part of the curves is investigated, it can be seen that the stiffness value is increasing proportionally with the number of fabric layers. 'V' shape in the curve of all specimens can be seen around 42 mm displacement values. This behavior may be associated with the damage pattern of the fabric in Figure 9. After the first load drop occurred, the fabric structure became bulkier, which increased the contact force again.

$$Absorbed\ energy = \int_0^{\delta} F.d\delta \quad (1)$$

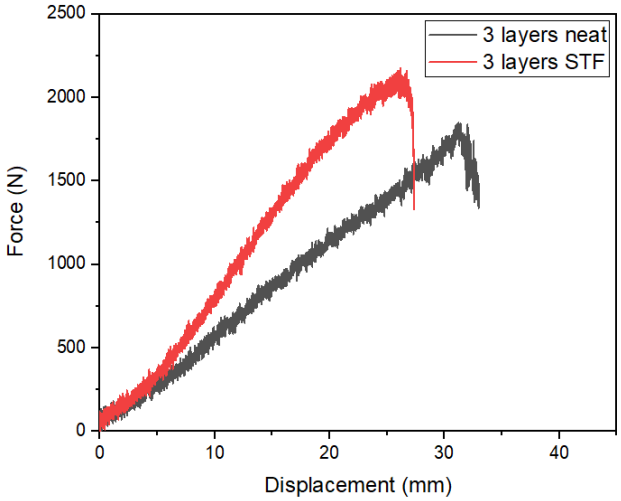

Figure 6. A comparison of low velocity impact response between neat aramid and STF impregnated aramid fabric for 3 layers specimens.

The amount of absorbed energy by fabric specimens was calculated by integrating under the area of the force-displacement curve as shown in Equation 1. Herein, 'F' is the contact force, and 'δ' is displacement. Calculated values were listed in Table 1 and plotted in Figure 8 to fit a curve. Table 1 also shows that maximum contact force values depend on the number of layers. The increasing rate of maximum contact force has decreased with the increasing number of layers. For instance, the ratio in contact force between 1-layer and 2-layers specimens is 1.92, while this value is 1.16 for 7- and 8-layers specimens. This situation can be explained by the fact that the rigidity of specimens does not increase critically after a certain level of layering.

Equation 2 is the curve-fitting equation, which shows the relationship between the number of layers and the amount of absorbed energy. In this equation, 'x' implies the number of layers, while 'y' represents absorbed energy.

Figure 9 presents the damage mechanisms and damage areas for a 2-layer STF-impregnated aramid fabric specimens. Two different damage zones were observed in specimens: primary and secondary. In the primary damage zone, both the geometrical pattern of the fabric and the fibers were subjected to damage, while in the secondary damage zone, only the geometrical distortion was distorted. Ruptured yarns on the right side of Figure 9 play a key role in mitigating impact energy.

Table 1. Relationship between number of fabric layers and energy absorption values

Number of layers	Absorbed Energy (J)	Maximum Contact Force (N)
1	16.3	487.13
2	24	935.34
3	40	1747.74
4	70	2715.76
5	90	3277.60
6	115	3851.87
7	150	4230.05
8	180	4888.37

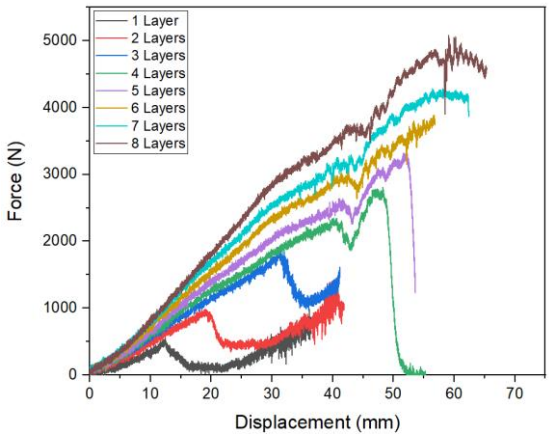

Figure 7. A comparison of low velocity impact response between neat aramid and STF impregnated aramid fabric for 3 layers specimens.

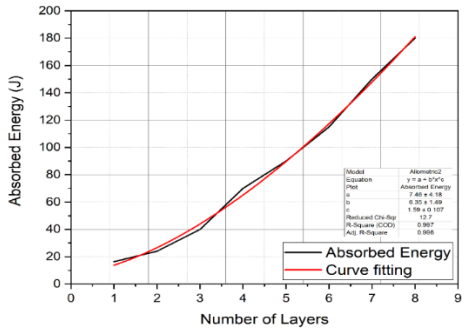

Figure 8. Curve fitting equation for relationship between absorbed energy and number of layers.

$$y = 7.46 + 6.35(x^{1.59}) \quad (2)$$

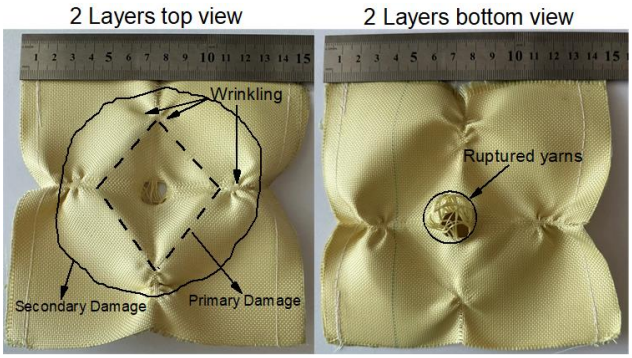

Figure 9. Damage mechanisms and regions for a 2 layers STF impregnated aramid fabric

4. Conclusion and Suggestions

Shear thickening fluids having 5%, 10%, and 20% silica concentrations were prepared and analysed by a rheometer to determine their thickening behaviors. There was a 15% difference in terms of the viscosity increase rate between 10% and 20% concentration solutions. Then, STF-impregnated aramid fabric specimens were examined by LVI test at different impact energies from 20 J to 240 J. Table 1 presents energy absorption, the number of layers relationship, and maximum contact force values. Finally, an equation in power function form (Eq.2) was obtained from Figure 8 as a curve-fitting equation. This relationship may be used for different energy absorption applications. As an example of the usage of this equation, a type IIA-level ballistic threat has a kinetic energy of around 555 J depending on ammo type- according to the NIJ 0101.06 standard. To absorb this level of kinetic energy, the needed number of fabric layers can be found at 16 layers.

Acknowledgment

This work was supported by Yalova University Scientific Research Projects Unit (BAP) (Project No: 2020/AP/0013). The author would like to express his thanks for funding.

Statement of Research and Publication Ethics

The study is complied with research and publication ethics.

References

[1] T. A. Hassan, V. K. Rangari, and S. Jeelani, "Synthesis, processing and characterization of shear thickening fluid (STF) impregnated fabric composites," *Materials Science and Engineering: A*, vol. 527, no. 12, pp. 2892-2899, 2010.

[2] A. Majumdar, B. S. Butola, and A. Srivastava, "Optimal designing of soft body armour materials using shear thickening fluid," *Materials & Design (1980-2015)*, vol. 46, pp. 191-198, 2013.

[3] A. Haris, H. P. Lee, T. E. Tay, and V. B. C. Tan, "Shear thickening fluid impregnated ballistic fabric composites for shock wave mitigation," *International Journal of Impact Engineering*, vol. 80, pp. 143-151, 2015.

[4] W. Na *et al.*, "Shear behavior of a shear thickening fluid-impregnated aramid fabrics at high shear rate," *Composites Part B: Engineering*, vol. 97, pp. 162-175, 2016.

[5] N. Asija, H. Chouhan, S. A. Gebremeskel, and N. Bhatnagar, "High strain rate characterization of shear thickening fluids using Split Hopkinson Pressure Bar technique," *International Journal of Impact Engineering*, vol. 110, pp. 365-370, 2017.

[6] S. Cao, Q. Chen, Y. Wang, S. Xuan, W. Jiang, and X. Gong, "High strain-rate dynamic mechanical properties of Kevlar fabrics impregnated with shear thickening fluid," *Composites Part A: Applied Science and Manufacturing*, vol. 100, pp. 161-169, 2017.

[7] M. Hasanzadeh, V. Mottaghitalab, M. Rezaei, and H. Babaei, "Numerical and experimental investigations into the response of STF-treated fabric composites undergoing ballistic impact," *Thin-Walled Structures*, vol. 119, pp. 700-706, 2017.

[8] A. Majumdar, A. Laha, D. Bhattacharjee, and I. Biswas, "Tuning the structure of 3D woven aramid fabrics reinforced with shear thickening fluid for developing soft body armour," *Composite Structures*, vol. 178, pp. 415-425, 2017.

[9] K. Fu, H. Wang, L. Chang, M. Foley, K. Friedrich, and L. Ye, "Low-velocity impact behaviour of a shear thickening fluid (STF) and STF-filled sandwich composite panels," *Composites Science and Technology*, vol. 165, pp. 74-83, 2018.

[10] K. Fu, H. Wang, S. Wang, L. Chang, L. Shen, and L. Ye, "Compressive behaviour of shear-thickening fluid with concentrated polymers at high strain rates," *Materials & Design*, vol. 140, pp. 295-306, 2018.

[11] A. Haris, H. P. Lee, and V. B. C. Tan, "An experimental study on shock wave mitigation capability of polyurea and shear thickening fluid based suspension pads," *Defence Technology*, vol. 14, no. 1, pp. 12-18, 2018.

[12] Q. He, S. Cao, Y. Wang, S. Xuan, P. Wang, and X. Gong, "Impact resistance of shear thickening fluid/Kevlar composite treated with shear-stiffening gel," *Composites Part A: Applied Science and Manufacturing*, vol. 106, pp. 82-90, 2018.

[13] X. Wu, K. Xiao, Q. Yin, F. Zhong, and C. Huang, "Experimental study on dynamic compressive behaviour of sandwich panel with shear thickening fluid filled pyramidal lattice truss core," *International Journal of Mechanical Sciences*, vol. 138-139, pp. 467-475, 2018.

[14] V. A. Chatterjee, S. K. Verma, D. Bhattacharjee, I. Biswas, and S. Neogi, "Enhancement of energy absorption by incorporation of shear thickening fluids in 3D-mat sandwich composite panels upon ballistic impact," *Composite Structures*, vol. 225, 2019.

[15] S. Sen, N. B. Jamal M, A. Shaw, and A. Deb, "Numerical investigation of ballistic performance of shear thickening fluid (STF)-Kevlar composite," *International Journal of Mechanical Sciences*, vol. 164, 2019.

[16] C. Caglayan, I. Osken, A. Ataalp, H. S. Turkmen, and H. Cebeci, "Impact response of shear thickening fluid filled polyurethane foam core sandwich composites," *Composite Structures*, vol. 243, 2020.

[17] L. Liu, Z. Yang, Z. Zhao, X. Liu, and W. Chen, "The influences of rheological property on the impact performance of kevlar fabrics impregnated with SiO2/PEG shear thickening fluid," *Thin-Walled Structures*, vol. 151, 2020.

[18] C. Huang, L. Cui, Y. Liu, H. Xia, Y. Qiu, and Q.-Q. Ni, "Low-velocity drop weight impact behavior of Twaron® fabric investigated using experimental and numerical simulations," *International Journal of Impact Engineering*, vol. 149, 2021.

[19] M. R. Sheikhi and S. Gürgen, "Anti-impact design of multi-layer composites enhanced by shear thickening fluid," *Composite Structures*, vol. 279, 2022.

[20] V. Mahesh, D. Harursampath, and V. Mahesh, "An experimental study on ballistic impact response of jute reinforced polyethylene glycol and nano silica based shear thickening fluid composite," *Defence Technology*, vol. 18, no. 3, pp. 401-409, 2022.

[21] C.-H. Shih, C.-P. Chang, Y.-M. Liu, Y.-L. Chen, and M.-D. Ger, "Ballistic Performance of Shear Thickening Fluids (STFs) Filled Paper Honeycomb Panel: Effects of Laminating Sequence and Rheological Property of STFs," *Applied Composite Materials*, vol. 28, no. 1, pp. 201-218, 2021.

[22] Y. S. Lee, E. D. Wetzel, and N. J. Wagner, "The ballistic impact characteristics of Kevlar woven fabrics impregnated with a colloidal shear thickening fluid," *Journal of Materials Science*, vol. 38, pp. 2825-2833, 2003.

[23] A. F. Ávila, A. M. de Oliveira, S. G. Leão, and M. G. Martins, "Aramid fabric/nano-size dual phase shear thickening fluid composites response to ballistic impact," *Composites Part A: Applied Science and Manufacturing*, vol. 112, pp. 468-474, 2018.

[24] S. Gürgen and M. C. Kuşhan, "The ballistic performance of aramid based fabrics impregnated with multi-phase shear thickening fluids," *Polymer Testing*, vol. 64, pp. 296-306, 2017.

[25] S. Gürgen, W. Li, and M. C. Kuşhan, "The rheology of shear thickening fluids with various ceramic particle additives," *Materials & Design*, vol. 104, pp. 312-319, 2016.

[26] A. Khodadadi, G. Liaghat, S. Vahid, A. R. Sabet, and H. Hadavinia, "Ballistic performance of Kevlar fabric impregnated with nanosilica/PEG shear thickening fluid," *Composites Part B: Engineering*, vol. 162, pp. 643-652, 2019.

[27] J. Qin, B. Guo, L. Zhang, T. Wang, G. Zhang, and X. Shi, "Soft armor materials constructed with Kevlar fabric and a novel shear thickening fluid," *Composites Part B: Engineering*, vol. 183, 2020.